Cardiovascular Hemodynamics in Mice with Tumor Necrosis Factor Receptor - Associated Factor 2 Mediated Cytoprotection in the Heart

Authors and Affiliations:

Andrea G. Marshall[1,*], Kit Neikirk[1,*], Zer Vue[1,*], Heather K. Beasley[1], Edgar Garza-Lopez[2], Larry Vang[1], Taylor Barongan[1], Zoe Evans[1], Josephs Anudokem, Jr.[1], Thuy T. Pham[3], Jose A. Gomez[4], Vernat Exil[5,6], Dao-fu Dai[7], Mark L. Entman[3], George E Taffet[3], Antentor O. Hinton, Jr[1,#], Anilkumar K. Reddy[3,#]

[1] Department of Molecular Physiology and Biophysics, Vanderbilt University, Nashville, TN, 37232, USA.
[2] Department of Internal Medicine, University of Iowa, Iowa City, IA, 52242, USA.
[3] Department of Medicine, Baylor College of Medicine, One Baylor Plaza, Houston, TX 77030, USA.
[4] Department of Medicine, Vanderbilt University Medical Center, Nashville, TN, 37232, USA
[5] Department of Pediatrics, Div. of Cardiology, St. Louis University School of Medicine, St. Louis, MO, 63104, USA.
[6] Department of Pediatrics, Carver College of Medicine, University of Iowa, Iowa City, IA. 52242, USA.
[7] Department of Pathology, Carver College of Medicine, University of Iowa, Iowa City, IA, 52242, USA.

Running Title: Cardiovascular Hemodynamics in TRAF2 Mice

Corresponding Authors

Anilkumar K. Reddy, Ph.D.
Department of Medicine
Baylor College of Medicine
One Baylor Plaza, MS: BCM285
Houston, TX 77030, USA.
Ph: 713-798-6831
Email: areddy@bcm.edu

Antentor O. Hinton, Jr, Ph.D.
Department of Molecular Physiology and Biophysics
Vanderbilt School of Medicine Basic Sciences
The Vanderbilt Diabetes Research and Training Center
750 Robinson Research Building
2200 Pierce Ave
Nashville, TN 37232-0615
319-383-3095 (cell)
antentor.o.hinton.jr@Vanderbilt.Edu

Abstract

Many studies in mice have demonstrated that cardiac-specific innate immune signaling pathways can be reprogrammed to modulate inflammation in response to myocardial injury and improve outcomes. In these studies, however, the standard parameters of left ventricular (LV) ejection fraction, fractional shortening, and end-diastolic diameter, among others, to assess cardiac function depend upon loading conditions and therefore do not completely reflect the contractile function of the heart. A true measure of global cardiac efficiency should include of the interaction between the ventricle and the aorta (ventriculo-vascular coupling, VVC) as well as measures of aortic impedance and pulse wave velocity. We measured cardiac Doppler velocities, blood pressures, along with VVC, aortic impedance, and pulse wave velocity to evaluate global cardiac function in mouse model of cardiac-restricted low levels TRAF2 overexpression that conferred cytoprotection in the heart. While response to myocardial infraction and reperfusion was improved in the TRAF2 overexpressed mice, we found that TRAF2 mice had significantly lower cardiac systolic velocities and accelerations, diastolic atrial velocity, lower aortic pressures and rate-pressure product, lower LV contractility and relaxation, and lower stroke work when compared to littermate control mice. Also, we found significantly longer aortic ejection time, isovolumic contraction and relaxation times, and significantly higher mitral early/atrial ratio, myocardial performance index, and ventricular vascular coupling in the TRAF2 overexpression mice compared to their littermate controls. We found no significant differences in the aortic impedance and pulse wave velocity. While the reported tolerance to ischemic insults in TRAF2 overexpression mice may suggest enhanced cardiac reserve, our results indicate a diminished cardiac function in these mice.

Keywords

Systolic and diastolic function, myocardial performance index, ventricular-vascular coupling, arterial and left ventricular elastance, aortic impedance

Introduction

Tumor Necrosis Factor (TNF) Receptor Associated Factor 2 (TRAF2), an E3 Ubiquitin-protein ligase, interacts with signaling molecules responsible for cell death, cellular stress response, activation of nuclear factor-*k*B and JNK (1, 2) and critical pathways for cellular senescence and regeneration (3). The TRAF2 pathway is activated by tumor necrosis factor and recruits for apoptosis inhibitor proteins, cIAP1/2 (4). Tumor necrosis factor can protect against ischemic-induced cardiomyocyte death (5). In contrast, its knockout is less cardioprotective (6, 7). In cancer studies it was shown that TRAF2 can act as both a tumor promotor and suppressor (8). Given such juxtaposing roles, it is not surprising that mixed outcomes have been reported on the role of TRAF2 as a potential downstream mediator of cardiac protection in heart failure. TNF is cytoprotective in the heart via TRAF2 mediated activation of NF-kB (9), TRAF2 mitochondrial localization is cytoprotective, and may also contribute to TRAF2-mediated mitophagy (10), and that TRAF2 mediates myocardial survival by suppressing apoptosis and necroptosis (11). These roles make TRAFs important targets in many inflammatory and autoimmune diseases (12). However, other studies have suggested that cardiac function was improved after myocardial infarction in absence of NF-kB p50 subunit (13), that suppressing NF-kB with oligonucleotide decoys reduces ischemia related myocardial injury (14), and that TRAF2 mediates enhanced cardiac hypertrophy via activation of AKT/GSK3β signaling (15). Regardless, overexpression of TRAF2 was found to have cardioprotective role in myocardial injury and perhaps can be novel therapeutic strategy in cardiomyopathy (16).

Most studies in mice use echocardiography measurements of LV ejection fraction (EF), fractional shortening (FS), and end-diastolic diameter (EDD), among others, to assess cardiac function much akin to those used clinical studies (17). But EF, FS, or EDD are dependent on loading conditions and not completely reflective of the contractile function of the heart (18). Therefore, it is important include the interaction between ventricle and the aorta (also known as, ventricular-vascular coupling, VVC) to evaluate the performance of LV as a true measure of global cardiovascular efficiency (17, 19). The VVC is determined as the ratio of aortic elastance (Ea) and end-systolic elastance (Ees) has recently been recommended for risk stratification for heart failure (20). The parameters, Ea and Ees may be less sensitive in disease, when more

sensitive parameters of myocardial longitudinal strain and aortic pulse wave velocity or aortic impedance may be used (20, 21).

In their study, Burchfield et al. (2010) mainly characterized the cardiac function to evaluate the effects of cardiac-restricted low levels TRAF2 overexpression (MHC-TRAF2$_{LC}$) in mice and concluded that TNF is cytoprotective in the heart via TRAF2 mediated activation of NF-kB. While the cardiac effects are known, there is a need to evaluate these animal models using measurements of VVC and aortic impedance to determine true global myocardial performance. Here we studied the same TRAF2 mouse model using cardiac systolic, diastolic, aortic and LV pressure, VVC, and aortic impedance to comprehensive characterization the global cardiovascular function (Figure 1).

Methods

Animals. The generation of MHC-TRAF2$_{LC}$ mice was previously described (9). Briefly, animals were generated with α-myosin heavy chain promoter targeting murine TRAF2. Histological analysis at 12 weeks was used to characterize the mice. We used 8 MHC-TRAF2$_{LC}$ (TRAF2) and 8 littermate controls (CTR) at 2-3 months of age. The diets of both groups of mice consisted of normal chow with free access to food and water. All animal protocols were approved by the Institutional Animal Care and Use Committee of Baylor College of Medicine in accordance with the National Institutes of Health Guide for the Care and Use of Laboratory Animals. Anesthesia was induced in mice with 2.5% isoflurane initially, transferred to a heated (37±1°C) electrocardiography board (MouseMonitor S, Indus Instruments, Webster, TX) with isoflurane maintained at 1.5%. The mouse paws were attached to electrodes to measure electrocardiogram (ECG).

Doppler flow velocity measurements. Cardiac Doppler aortic outflow velocity and mitral inflow signals were measured with 10 MHz Doppler probe with all signals (including blood pressure and ECG) were simultaneously acquired using Doppler Flow Velocity System (DFVS; Indus Instruments, Webster, TX). From the cardiac Doppler signals, we calculated peak (Vp) and mean (Vm) aortic velocities, stroke distance (Sd), ejection time (ET), peak (Ap) and mean (Am) aortic accelerations, Mitral early peak (E) and atrial peak (A) velocities, E/A ratio, deceleration time

(DT) isovolumic contraction (IVCT) & relaxation (IVRT) times, and myocardial performance index (MPI - also known as Tei index).

Blood pressure and flow velocity measurements. Blood pressure measurements were made as previously described (22, 23). Briefly, the right carotid artery was isolated and cannulated with a pressure catheter (SPR-1000: Millar Instruments, Inc., Houston, TX) and advanced into the ascending aorta to measure aortic pressure (along with simultaneous measurement aortic blood flow velocity as described below). The aortic pressure and velocity signals were displayed simultaneously, a 2-s segments of both signals were recorded using DFVS system. The catheter was then advanced into the LV. Again, 2-s segments of LV pressure. Systolic (SBP), diastolic (DBP), mean (MBP), pulse pressures (PP), and rate-pressure product (RPP) were calculated from aortic pressure. Peak LV pressure (P_{LVP}), indices of contractility ($+dP/dt_{max}$) and relaxation ($-dP/dt_{max}$), relaxation time constant (tau), and LV end diastolic pressure (LVEDP) were calculated from LV pressure.

Determination of aortic input impedance. Aortic input impedance was determined using previously reported methods (22–25). Briefly, impedance was determined using the simultaneously measured ascending aortic pressure and velocity signals. The pressure and velocity waveforms were processed using discrete Fourier transform to determine aortic input impedance (Zi). Peripheral vascular resistance (Zp – impedance at zero frequency), impedance at first harmonic (Z_1), characteristic impedance (Zc – average of 2nd to 10th harmonic) were extracted from modulus of aortic impedance (|Zi|). Pulse wave velocity was calculated from |Zi| as Zc/ρ (ρ - density of blood).

Calculation of parameters to determine VVC. Arterial elastance (Ea) was calculated as ESP/SV (stroke volume, SV=Sd*aortic cross-sectional area), end systolic elastance (Ees) was calculated as ESP/ESV, ventricular-vascular coupling (VVC) was calculated as Ea/Ees, and stroke work (SW) was calculated as ESP*SV (17).

Statistical analyses. All the data are presented as mean ± standard error of the mean (SEM). Statistical analyses were performed via analysis using Student's T-test on Prism (GraphPad Software; La Jolla, USA).

Results

The general physiological parameters were measured in TRAF2 mice and compared to CTR mice. Body weight (BW), aortic cross-sectional area (ACA), and heart rate (HR) were unaffected with TRAF2 overexpression (Figure 2A-C). We determined the impact of TRAF2 overexpression on cardiac systolic function and found a significant decrease in peak aortic velocity (Vp), mean aortic velocity (Vm), and stroke distance (Sd) in TRAF2 mice compared to CTR mice (Figure 3A-C). We also found a significant increase in aortic ejection time (ET) (Figure 3D) and significant decreases in both peak (Ap) and mean (Am) acceleration in TRAF2 mice (Figure 3F-G).

While there were no significant differences in mitral peak early (E) velocity, peak atrial (A) velocity decreased significantly, resulting in the near doubling of Peak E/A ratio (Figure 4A-C). We observed significant decrease in E-deceleration time (DT) and significant increases in both isovolumetric relaxation (IVRT) and contraction time (IVCT) with TRAF2 overexpression (Figure 4D-F). Myocardial performance index (MPI, also known as Tei Index) increased significantly TRAF2 mice compared to CTR mice (Figure 3G).

Systolic blood pressure (SBP) showed a significant decrease with TRAF2 overexpression, while diastolic blood pressure (DBP) showed a slight decrease, but it was not statistically significant (Figure 5A-B). Also, mean blood pressure (MBP), pulse pressure (PP=SBP-DBP), and rate pressure product (RPP=SBP*HR) all decreased significantly decrease in TRAF2 mice compared to the CTR mice (Figure 5C-E).

While peak left ventricular pressure (P_{LVP}) was lower in the TRAF2 mice it was not significantly different from CTR mice (Figure 6A), both $+dP/dt_{max}$ and $-dP/dt_{max}$ were significantly lower in TRAF2 mice compared to CTR mice (Figure 6B-C). The relaxation time constant (tau) and LV end diastolic pressure (P_{LVED}) trended higher but were not significantly different in TRAF2 overexpression mice compared to CTR mice (Figure 6D-E).

There were no differences in arterial elastance (Ea) but end systolic LV elastance (Ees) was significantly lower in TRAF2 mice, resulting in ventricular-vascular coupling to be significantly

higher in TRAF2 mice (Figure 7A-C). Also, stroke work was significantly lower in the TRAF2 mice when compared to CTR mice (Figure 7D)

LV afterload was evaluated using aortic impedance. We found no significant differences in any of the impedance parameters, Zp, Z_1, Zc (or PWVz) between the two groups (Figure 8A-D).

Discussion

Previous study by our group suggested a TRAF2 cardioprotective function (9). As an extension of this previous study, we currently evaluated the cardiac and aortic hemodynamics to comprehensively characterize cardiovascular function in the cardiac-restricted low-level overexpression of TRAF2 (MHC-$TRAF2_{LC}$) mouse model. We wanted to determine if ventricular-vascular coupling (a measure of cardiac global efficiency) and the arterial hemodynamics were different or influenced/contributed to the cardioprotective function in the TRAF2 mouse model. We made measurements of aortic and left ventricular blood pressure measurements along with cardiac inflow and outflow velocity measurements. The general parameters of body weight, aortic cross-sectional area, and heart rate of TRAF2 overexpressing mice were not significantly different from CTR mice (Figure 2).

Cardiac systolic and diastolic function. We found that the cardiac systolic function, as determined by peak and mean aortic flow velocities, peak and mean aortic accelerations (Figure 3) and $+dP/dt_{max}$ (Figure 4), is diminished in TRAF2 mice compared to the CTR mice which may indicate a mild systolic dysfunction or enhanced systolic reserve. The LV pressure indices of contractility ($+dP/dt_{max}$) and relaxation ($-dP/dt_{max}$) were significantly lower in the TRAF2 mice and followed a similar trend that was observed in the aortic blood pressure and velocity and in agreement with decrease in %FS reported by Burchfield et al. (2010) Again, these diminished contractile and relaxation function in TRAF2 mice are similar to what we observed in the young dwarf *Little* mice (26). We have not challenged these mice to determine systolic reserve capacity, but our group showed that left ventricular developed pressure recovered better in the TRAF2 mice after IR injury and observed that the cytoprotective effects of TRAF2 were mediated by NF-κB activation (9). But others have reported that suppression of NF-kB with oligonucleotide transcription factor decoys diminishes ischemia related myocardial injury (14) and that cardiac

function improved after myocardial infarction with absence of NF-kB p50 unit (13). However, our group reiterated the cytoprotective effects of TRAF2 may have been afforded via crosstalk between canonical and noncanonical NF-kB signaling pathways (27). A more recent study noted that TRAF2 maintains myocardial homeostasis through facilitation of cardiac myocyte mitophagy thus preventing inflammation and cell death (16). We also found that aortic ejection time were significantly prolonged in the TRAF2 mice (Figure 3D). Obata et al. (2017) reported that longer aortic ejection time is associated with lower blood pressures (28), and perhaps the low blood pressures in TRAF2 mice in our study may have caused longer ejection times. Also, longer ET results from longer action potential duration in old animals and may be associated with cellular changes in the mechanics of excitation–contraction coupling (29). Similar cellular changes may be present in TRAF2 that could have caused prolonged ejection time.

The cardiac diastolic function, as defined by E/A ratio was higher in TRAF2 mice than CTR mice (Figure 4C) indicating improved diastolic function. However, E>>A (or E/A>2) and shorter E-deceleration time is associated with moderate decrease in compliance (30). The TRAF2 mice had E/A>2 and shorter E-deceleration time (Figure 4D) perhaps indicating a decline in compliance which agrees with the observation by Burchfield et al., (2010) that TRAF2 mice had mildly hypertrophic hearts (9). Isovolumic contraction time is index of LV contractility and isovolumic relaxation time is an index of LV relaxation, but both are dependent on heart rate (31) and other factors. Prolonged IVRT indicates impaired relaxation and prolonged IVCT is associated with reduced EF, both increasing the risk for heart failure (32). Since IVCT and IVRT are both associated with LV ejection time, the myocardial performance index (MPI or Tei Index) provides an overall cardiac performance (31). We found that TRAF2 overexpression resulted a small but significant increase in MPI index (Figure 4G) which may indicate impaired cardiac function like that reported in patients (33).

While TRAF2 overexpression confers cardioprotective effects, the small but significant changes in the systolic and diastolic parameters indicate a modest decrease in baseline function. It remains to be seen if this diminished function deteriorates with age or remains stable over their life span like that in the dwarf *Little* mice which maintain a diminished but stable cardiac function over their life span (26).

Aortic and LV Pressure. TRAF2 in mice had significantly lower systolic, mean, and pulse pressures compared to CTR mice. The lower blood pressures combined with lower blood velocities in TRAF2 mice make LV afterload appear normal in these mice. Previous studies reported that every 20 or 10 mmHg increase in SBP or DBP, respectively, beyond traditionally healthy values (34) doubles the chance of major long-term consequences of such as heart failure or stroke (35). Since SBP remains a stronger indicator of cardiovascular health than DBP at ages over 50, our findings suggests that the cardioprotective effects of TRAF2 potentially may be conferred across aging (36). Also, pulse pressure that is ≤25% of systolic pressure is considered too low and typically occurs in aortic stenosis, cardiac tamponade, aortic stenosis, or with blood loss (37). Pulse pressure in TRAF2 mice was ≈25% of systolic pressure perhaps indicating modest dysfunction. Given that we measured blood pressure in these mice at young age, studies at older ages may reveal if cardioprotective effects of TRAF2 overexpression are maintained across life span. The rate pressure product (RPP = SBP x heart rate), which is an indirect measurement of the heart oxygen consumption (38), was significantly lower in TRAF2 mice than CTR mice indicating a lower heart workload.

Ventricular-Vascular Coupling. A measure of myocardial performance that include interaction with aortic function, the ventricular-vascular coupling (VVC) was significantly higher in the TRAF2 mice indicating a diminished global cardiovascular efficiency. While aortic elastance was unchanged, the higher VVC in TRAF2 mice was mainly due to significantly lower end-systolic LV elastance. Similar observations were made in patients with major adverse cardiovascular events (17). Also, it has been shown that decreased LV stroke work index is associated with diminished LV systolic and diastolic function in cardiac intensive care unit patients (39). Also, we found that stroke work is significantly lower in the in the TRAF2 mice perhaps indicating a diminished cardiac function.

Aortic Impedance. Defined as the ratio of modulus of pressure to modulus of velocity at several harmonics (0-10) in frequency domain, aortic impedance provides comprehensive description of the afterload experienced by the left ventricle. This includes the pulsatile and the steady components of the hydraulic load compared with when pressure and velocity are considered individually (23, 24, 40). We used blood flow velocity instead of volume flow because both blood flow velocity and pressure are independent of body weight or size (24). We found that the

peripheral vascular resistance (represented by impedance modulus at 0, Zp), impedance at the first harmonic (Z_1) which correlates with the strength of the wave reflections from the periphery, characteristic impedance (Zc; average of 2-10 harmonics) which represents the pulsatile component of the aortic pressure-velocity relationship determined by local aortic wall stiffness and diameter and aortic stiffness index, pulse wave velocity (PWV), derived from Zc were not different in TRAF2 mice when compared to CTR mice. The unchanged Zc & PWV_{Zc} seems to conflict with our finding that pulse pressure was lower in TRAF2 mice. While PWV is a direct measure of aortic stiffness, pulse pressure is used as a surrogate stiffness index that also reflects stroke volume (which was also lower in TRAF2 mice) and both measures (stiffness & pulse pressure) are mildly correlated (41). In another study anti-hypertensive treatments in patients resulted in no changes in aortic PWV but had significant decrease in brachial pulse pressure (42). Again, these observations are made in these mice at young age and the effectiveness of TRAF2 mediated cytoprotection of the heart and cardiovascular system with age needs to be investigated.

Conclusions

Previous studies suggest that TRAF2 overexpression may confer cytoprotection of the heart and perhaps afford a potentially important therapeutic target for CVD treatment. However, examination of the global cardiovascular function revealed a diminished cardiac function in the mice with TRAF2 overexpression but there are no differences in the aortic impedance implying no increased afterload. The diminished cardiac function in these mice and the apparent tolerance to ischemic insults may suggest that their cardiovascular reserve may be enhanced. The observations reported by us, and others were from findings in in 2-3 month old mice and perhaps studies need to be conducted at older ages to determine if the cardioprotective effects of TRAF2 overexpression are maintained across life span without significant deterioration of cardiac function.

Acknowledgement:

We like to thank Dr. Douglas L Mann, MD (Professor, Washington University School of Medicine, St. Louis) for providing us the TRAF2 overexpression mice and their littermates.

FUNDING

This work is supported by DeBakey Heart Center, National Institute of Aging grant AG-059599 & AG-059599-04S1 (to M.L. Entman); National Institute of Health (NIH) NIDDK T-32, number DK007563 entitled Multidisciplinary Training in Molecular Endocrinology to Z.V.; The United Negro College Fund/Bristol-Myers Squibb E.E. Just Faculty Fund, Burroughs Wellcome Fund Career Awards at the Scientific Interface Award, Burroughs Wellcome Fund Ad-hoc Award, National Institutes of Health Small Research Pilot Subaward to 5R25HL106365-12 from the National Institutes of Health PRIDE Program, DK020593, Vanderbilt Diabetes and Research Training Center for DRTC Alzheimer's Disease Pilot & Feasibility Program to A.H.J. Its contents are solely the responsibility of the authors and do not necessarily represent the official view of the NIH. The funders had no role in study design, data collection and analysis, decision to publish, or preparation of the manuscript.

Disclosures

Dr. Reddy is a collaborator and consultant with Indus Instruments, Webster, TX. All other authors have no competing interests.

Author Contributions

AGM - 3456, KN - 346, ZV - 3456, HKB - 34, EG - 34, LV - 34, TB - 34, ZE - 34, JA - 34, TTP - 23, JAG - 678, VE - 678, DD - 678, MLE - 7,8, GET - 5678, AOH - 5678, AKR - 12345678

1 Conceived and designed research, 2 Performed experiments and Data collection, 3 Data analysis, 4 Prepared figures, 5 Interpretation of results, 6 Drafted manuscript, 7 Edited and revised manuscript, 8 Approved final version of manuscript.

References

1. Bradley JR, Pober JS. Tumor necrosis factor receptor-associated factors (TRAFs). *Oncogene* 20: 6482–6491, 2001. doi: 10.1038/sj.onc.1204788.

2. Wajant H, Scheurich P. Tumor necrosis factor receptor-associated factor (TRAF) 2 and its role in TNF signaling. *The International Journal of Biochemistry & Cell Biology* 33: 19–32, 2001. doi: 10.1016/S1357-2725(00)00064-9.

3. Yarza R, Vela S, Solas M, Ramirez MJ. c-Jun N-terminal Kinase (JNK) Signaling as a Therapeutic Target for Alzheimer's Disease [Online]. *Frontiers in Pharmacology* 6, 2016. https://www.frontiersin.org/articles/10.3389/fphar.2015.00321 [28 Jul. 2022].

4. Gough P, Myles IA. Tumor Necrosis Factor Receptors: Pleiotropic Signaling Complexes and Their Differential Effects [Online]. *Frontiers in Immunology* 11, 2020. https://www.frontiersin.org/articles/10.3389/fimmu.2020.585880 [28 Jul. 2022].

5. Miao K, Zhou L, Ba H, Li C, Gu H, Yin B, Wang J, Yang X, Li Z, Wang DW. Transmembrane tumor necrosis factor alpha attenuates pressure-overload cardiac hypertrophy via tumor necrosis factor receptor 2. *PLOS Biology* 18: e3000967, 2020. doi: 10.1371/journal.pbio.3000967.

6. Benjafield AV, Wang XL, Morris BJ. Tumor necrosis factor receptor 2 gene (TNFRSF1B) in genetic basis of coronary artery disease. *J Mol Med* 79: 109–115, 2001. doi: 10.1007/s001090000168.

7. Higuchi Y, McTiernan CF, Frye CB, McGowan BS, Chan TO, Feldman AM. Tumor Necrosis Factor Receptors 1 and 2 Differentially Regulate Survival, Cardiac Dysfunction, and Remodeling in Transgenic Mice With Tumor Necrosis Factor-α–Induced Cardiomyopathy. *Circulation* 109: 1892–1897, 2004. doi: 10.1161/01.CIR.0000124227.00670.AB.

8. Siegmund D, Wagner J, Wajant H. TNF Receptor Associated Factor 2 (TRAF2) Signaling in Cancer. *Cancers (Basel)* 14: 4055, 2022. doi: 10.3390/cancers14164055.

9. Burchfield JS, Dong J-W, Sakata Y, Gao F, Tzeng H-P, Topkara VK, Entman ML, Sivasubramanian N, Mann DL. The cytoprotective effects of tumor necrosis factor are conveyed through tumor necrosis factor receptor-associated factor 2 in the heart. *Circ Heart Fail* 3: 157–164, 2010. doi: 10.1161/CIRCHEARTFAILURE.109.899732.

10. Yang K-C, Ma X, Liu H, Murphy J, Barger PM, Mann DL, Diwan A. Tumor Necrosis Factor Receptor–Associated Factor 2 Mediates Mitochondrial Autophagy. *Circulation: Heart Failure* 8: 175–187, 2015. doi: 10.1161/CIRCHEARTFAILURE.114.001635.

11. Guo X, Yin H, Li L, Chen Y, Li J, Doan J, Steinmetz R, Liu Q. Cardioprotective Role of Tumor Necrosis Factor Receptor-Associated Factor 2 by Suppressing Apoptosis and Necroptosis. *Circulation* 136: 729–742, 2017. doi: 10.1161/CIRCULATIONAHA.116.026240.

12. So T. The immunological significance of tumor necrosis factor receptor-associated factors (TRAFs). *International Immunology* 34: 7–20, 2022. doi: 10.1093/intimm/dxab058.

13. Frantz S, Hu K, Bayer B, Gerondakis S, Strotmann J, Adamek A, Ertl G, Bauersachs J. Absence of NF-kappaB subunit p50 improves heart failure after myocardial infarction. *FASEB J* 20: 1918–1920, 2006. doi: 10.1096/fj.05-5133fje.

14. Tranter M, Liu Y, He S, Gulick J, Ren X, Robbins J, Jones WK, Reineke TM. In vivo delivery of nucleic acids via glycopolymer vehicles affords therapeutic infarct size reduction in vivo. *Mol Ther* 20: 601–608, 2012. doi: 10.1038/mt.2011.267.

15. Huang Y, Wu D, Zhang X, Jiang M, Hu C, Lin J, Tang J, Wu L. Cardiac-specific Traf2 overexpression enhances cardiac hypertrophy through activating AKT/GSK3β signaling. *Gene* 536: 225–231, 2014. doi: 10.1016/j.gene.2013.12.052.

16. Ma X, Rawnsley DR, Kovacs A, Islam M, Murphy JT, Zhao C, Kumari M, Foroughi L, Liu H, Qi K, Diwan A, Hyrc K, Evans S, Satoh T, French BA, Margulies KB, Javaheri A, Razani B, Mann DL, Mani K, Diwan A. TRAF2, an Innate Immune Sensor, Reciprocally

Regulates Mitophagy and Inflammation to Maintain Cardiac Myocyte Homeostasis. *JACC Basic Transl Sci* 7: 223–243, 2022. doi: 10.1016/j.jacbts.2021.12.002.

17. Tona F, Zanatta E, Montisci R, Muraru D, Beccegato E, De Zorzi E, Benvenuti F, Civieri G, Cozzi F, Iliceto S, Doria A. Higher Ventricular-Arterial Coupling Derived from Three-Dimensional Echocardiography Is Associated with a Worse Clinical Outcome in Systemic Sclerosis. *Pharmaceuticals (Basel)* 14: 646, 2021. doi: 10.3390/ph14070646.

18. Park JJ, Park J-B, Park J-H, Cho G-Y. Global Longitudinal Strain to Predict Mortality in Patients With Acute Heart Failure. *J Am Coll Cardiol* 71: 1947–1957, 2018. doi: 10.1016/j.jacc.2018.02.064.

19. Asanoi H, Sasayama S, Kameyama T. Ventriculoarterial coupling in normal and failing heart in humans. *Circ Res* 65: 483–493, 1989. doi: 10.1161/01.res.65.2.483.

20. Ikonomidis I, Aboyans V, Blacher J, Brodmann M, Brutsaert DL, Chirinos JA, De Carlo M, Delgado V, Lancellotti P, Lekakis J, Mohty D, Nihoyannopoulos P, Parissis J, Rizzoni D, Ruschitzka F, Seferovic P, Stabile E, Tousoulis D, Vinereanu D, Vlachopoulos C, Vlastos D, Xaplanteris P, Zimlichman R, Metra M. The role of ventricular-arterial coupling in cardiac disease and heart failure: assessment, clinical implications and therapeutic interventions. A consensus document of the European Society of Cardiology Working Group on Aorta & Peripheral Vascular Diseases, European Association of Cardiovascular Imaging, and Heart Failure Association. *Eur J Heart Fail* 21: 402–424, 2019. doi: 10.1002/ejhf.1436.

21. Alhakak AS, Teerlink JR, Lindenfeld J, Böhm M, Rosano GMC, Biering-Sørensen T. The significance of left ventricular ejection time in heart failure with reduced ejection fraction. *Eur J Heart Fail* 23: 541–551, 2021. doi: 10.1002/ejhf.2125.

22. Reddy AK, Taffet GE, Li Y-H, Lim S-W, Pham TT, Pocius JS, Entman ML, Michael LH, Hartley CJ. Pulsed Doppler signal processing for use in mice: applications. *IEEE Transactions on Biomedical Engineering* 52: 1771–1783, 2005. doi: 10.1109/TBME.2005.855709.

23. Hinton Jr AO, Yang Y, Quick AP, Xu P, Reddy CL, Yan X, Reynolds CL, Tong Q, Zhu L, Xu J, Wehrens XHT, Xu Y, Reddy AK. SRC-1 Regulates Blood Pressure and Aortic Stiffness in Female Mice. *PLOS ONE* 11: e0168644, 2016. doi: 10.1371/journal.pone.0168644.

24. Reddy AK, Li Y-H, Pham TT, Ochoa LN, Treviño MT, Hartley CJ, Michael LH, Entman ML, Taffet GE. Measurement of aortic input impedance in mice: effects of age on aortic stiffness. *American Journal of Physiology-Heart and Circulatory Physiology* 285: H1464–H1470, 2003. doi: 10.1152/ajpheart.00004.2003.

25. Reddy AK, Hartley CJ, Pham TT, Darlington G, Entman ML, Taffet GE. Young Little Mice Express a Premature Cardiovascular Aging Phenotype. *The Journals of Gerontology: Series A* 69A: 152–159, 2014. doi: 10.1093/gerona/glt055.

26. Reddy AK, Amador-Noguez D, Darlington GJ, Scholz BA, Michael LH, Hartley CJ, Entman ML, Taffet GE. Cardiac function in young and old Little mice. *J Gerontol A Biol Sci Med Sci* 62: 1319–1325, 2007. doi: 10.1093/gerona/62.12.1319.

27. Evans S, Tzeng H-P, Veis DJ, Matkovich S, Weinheimer C, Kovacs A, Barger PM, Mann DL. TNF receptor-activated factor 2 mediates cardiac protection through noncanonical NF-κB signaling. *JCI Insight* 3: 98278, 2018. doi: 10.1172/jci.insight.98278.

28. Obata Y, Mizogami M, Singh S, Nyhan D, Berkowitz DE, Steppan J, Barodka V. Ejection time: influence of hemodynamics and site of measurement in the arterial tree. *Hypertens Res* 40: 811–818, 2017. doi: 10.1038/hr.2017.43.

29. WS Aranow. Cardiovascular System. In: *Encyclopedia of Gerontology*, edited by JE Birren. Elsevier, 2007, p. 224–229.

30. Oh JK, Seward JB, Tajik A. Assessment of diastolic function and diastolic heart failure. In: *Echo manual, The, 3rd edition, Lippincott Williams and Wilkins*. Rochester, MN: Lippincott Williams & Wilkins, 2006.

31. Tei C, Nishimura RA, Seward JB, Tajik AJ. Noninvasive Doppler-derived myocardial performance index: correlation with simultaneous measurements of cardiac catheterization

measurements. *J Am Soc Echocardiogr* 10: 169–178, 1997. doi: 10.1016/s0894-7317(97)70090-7.

32. Alhakak AS, Møgelvang R, Schnohr P, Modin D, Brainin P, Gislason G, Biering-Sørensen T. The cardiac isovolumetric contraction time is an independent predictor of incident heart failure in the general population. *Int J Cardiol* 312: 81–86, 2020. doi: 10.1016/j.ijcard.2020.03.046.

33. Harjai KJ, Scott L, Vivekananthan K, Nunez E, Edupuganti R. The Tei index: a new prognostic index for patients with symptomatic heart failure. *J Am Soc Echocardiogr* 15: 864–868, 2002. doi: 10.1067/mje.2002.120892.

34. A Randomized Trial of Intensive versus Standard Blood-Pressure Control. *N Engl J Med* 377: 2506, 2017. doi: 10.1056/NEJMx170008.

35. Gebremichael GB, Berhe KK, Zemichael TM. Uncontrolled hypertension and associated factors among adult hypertensive patients in Ayder comprehensive specialized hospital, Tigray, Ethiopia, 2018. *BMC Cardiovascular Disorders* 19: 121, 2019. doi: 10.1186/s12872-019-1091-6.

36. Kjeldsen SE. Hypertension and cardiovascular risk: General aspects. *Pharmacological Research* 129: 95–99, 2018. doi: 10.1016/j.phrs.2017.11.003.

37. Homan TD, Bordes S, Cichowski E. Physiology, pulse pressure. .

38. Nagpal S, Walia L, Lata H, Sood N, Ahuja GK. Effect of exercise on rate pressure product in premenopausal and postmenopausal women with coronary artery disease. *Indian J Physiol Pharmacol* 51: 279–283, 2007.

39. Jentzer JC, Wiley BM, Anavekar NS. Echocardiographic left ventricular stroke work index: An integrated noninvasive measure of shock severity. *PLoS One* 17: e0262053, 2022. doi: 10.1371/journal.pone.0262053.

40. Vlachopoulos C, O'Rourke M, Nichols WW. *McDonald's blood flow in arteries: theoretical, experimental and clinical principles*. CRC press, 2011.

41. Waldstein SR, Rice SC, Thayer JF, Najjar SS, Scuteri A, Zonderman AB. Pulse pressure and pulse wave velocity are related to cognitive decline in the Baltimore Longitudinal Study of Aging. *Hypertension* 51: 99–104, 2008. doi: 10.1161/HYPERTENSIONAHA.107.093674.

42. Mackenzie IS, McEniery CM, Dhakam Z, Brown MJ, Cockcroft JR, Wilkinson IB. Comparison of the effects of antihypertensive agents on central blood pressure and arterial stiffness in isolated systolic hypertension. *Hypertension* 54: 409–413, 2009. doi: 10.1161/HYPERTENSIONAHA.109.133801.

Figure Legend:

Figure 1: Workflow of the experimental setup to measure aortic blood flow velocity, aortic blood pressure and ECG (electrocardiogram) in TRAF2 and control mice.

Figure 2: General parameters of male wild type mice and MHC-TRAF2$_{LC}$ mice. (A) Body weight in grams, (B) aortic cross-sectional area, and (C) heart rate (HR) in beats per minute are shown. Data are presented as mean±SEM (n = 8/group). Ns indicates statistically non-significant relationship.

Figure 3: Aortic flow velocity indices of male wild type mice and MHC-TRAF2$_{LC}$ mice. (A) Peak aortic outflow velocity, (B) mean outflow velocity, (C) stroke distance, (D) aortic ejection time, (E) peak aortic outflow acceleration, and (F) mean aortic outflow acceleration. Data are presented as mean±SEM (n = 8/group). *,#, and § represents $p < 0.05$, $p < 0.01$, and $p < 0.001$, respectively.

Figure 4: Mitral flow velocity indices of male wild type mice and MHC-TRAF2$_{LC}$ mice. (A) peak mitral-early (E) flow velocity, (B) peak mitral-atrial (A) flow velocity, (C) mitral E/A ratio, (D) E-deceleration time, (E) isovolumic relaxation time, (F) isovolumic contraction time, and (G) myocardial performance index (Tei index), a measure of combined diastolic and systolic function, determined by the sum of isovolumetric relation and contraction time normalized against ejection time. All measurements obtained from cardiac Doppler flow velocity signals in

mice. Data are presented as mean±SEM (n = 8/group). * and # represents $p < 0.05$ and $p < 0.01$, respectively. Ns indicates statistically non-significant relationship.

Figure 5: Aortic blood pressure and rate pressure product of male wild type mice and MHC-$TRAF2_{LC}$ mice. (A) Systolic blood pressure (SBP), (B) Diastolic blood pressure (DBP), (C) Mean blood pressure (MBP), (D) Pulse pressure, and (E) Rate pressure product (RPP). Data are presented as mean±SEM (n = 8/group). *,#, and § represents $p < 0.05$, $p < 0.01$, and $p < 0.001$, respectively. Ns indicates statistically non-significant relationship.

Figure 6: Left ventricular blood pressure parameters of male wild type mice and MHC-$TRAF2_{LC}$ mice. (A) Peak left ventricular pressure (P_{LVP}), (B) Maximal contractility ($+dP/dt_{max}$), (C) Maximal relaxation ($-dP/dt_{max}$), (D) left ventricular end diastolic pressure (P_{LVED}), and (E) relaxation time constant (tau). Data are presented as mean±SEM (n = 8/group). * and # represents $p < 0.05$ and $p < 0.01$, respectively. Ns indicates statistically non-significant relationship.

Figure 7: Ventricular-vascular coupling. (A) aortic elastance, (B) end-systolic LV elastance, (C) ventricular-vascular coupling, and (D) stroke work. # represents $p < 0.01$, and Ns indicates statistically non-significant relationship.

Figure 8: Parameters of aortic impedance in male wild type mice and MHC-$TRAF2_{LC}$ mice. (A) Total peripheral resistance (Z_P), (B) impedance at first harmonic (Z_1), (C) characteristic impedance, (Z_C) (D), and impedance-based pulse wave velocity (PWV). Data are presented as mean±SEM (n = 8/group). Ns indicates statistically non-significant relationship.

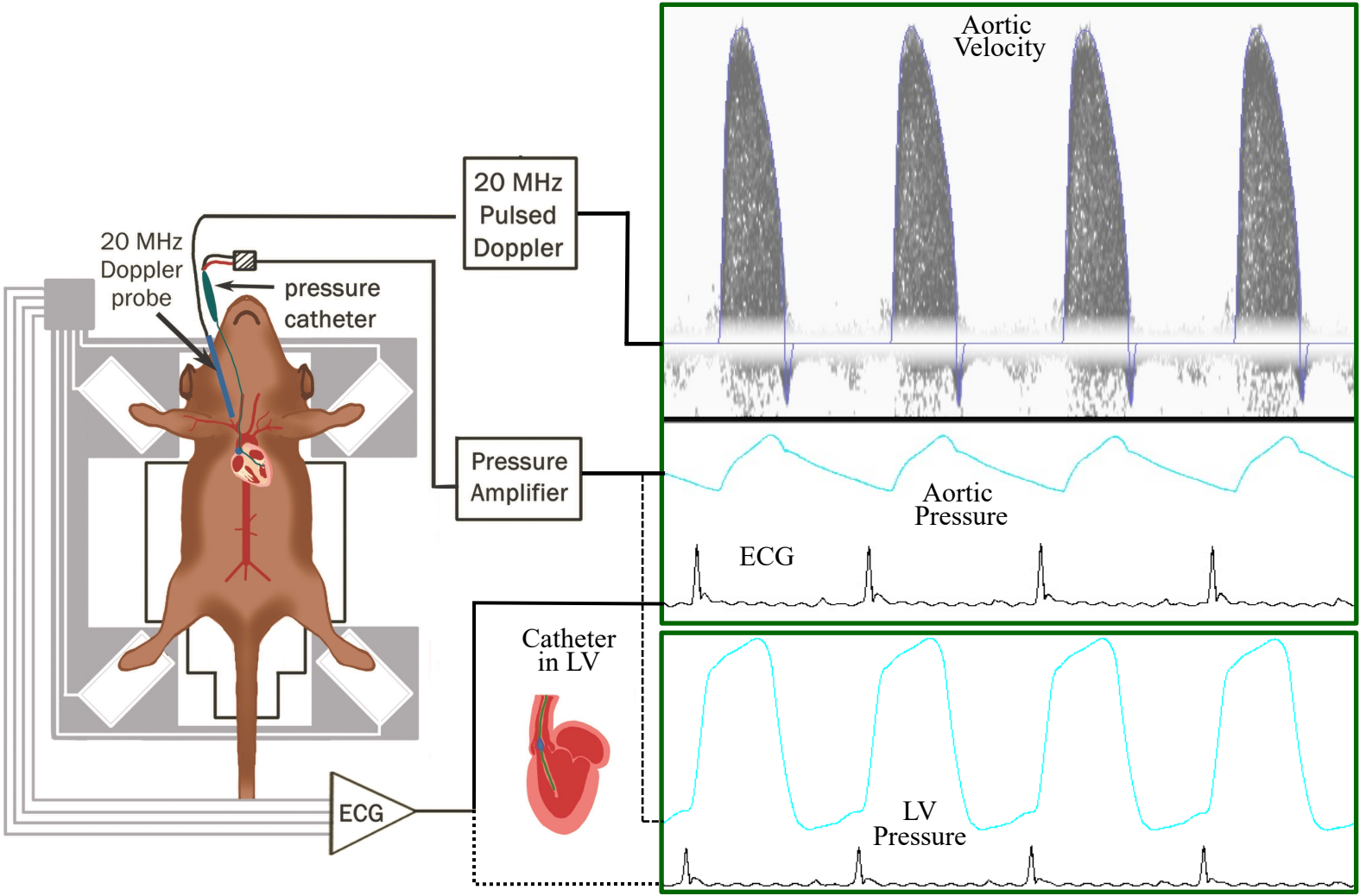
20 MHz
Doppler
probe
pressure
catheter
20 MHz
Pulsed
Doppler
Pressure
Amplifier
ECG
Catheter
in LV
Aortic
Velocity
Aortic
Pressure
ECG
LV
Pressure

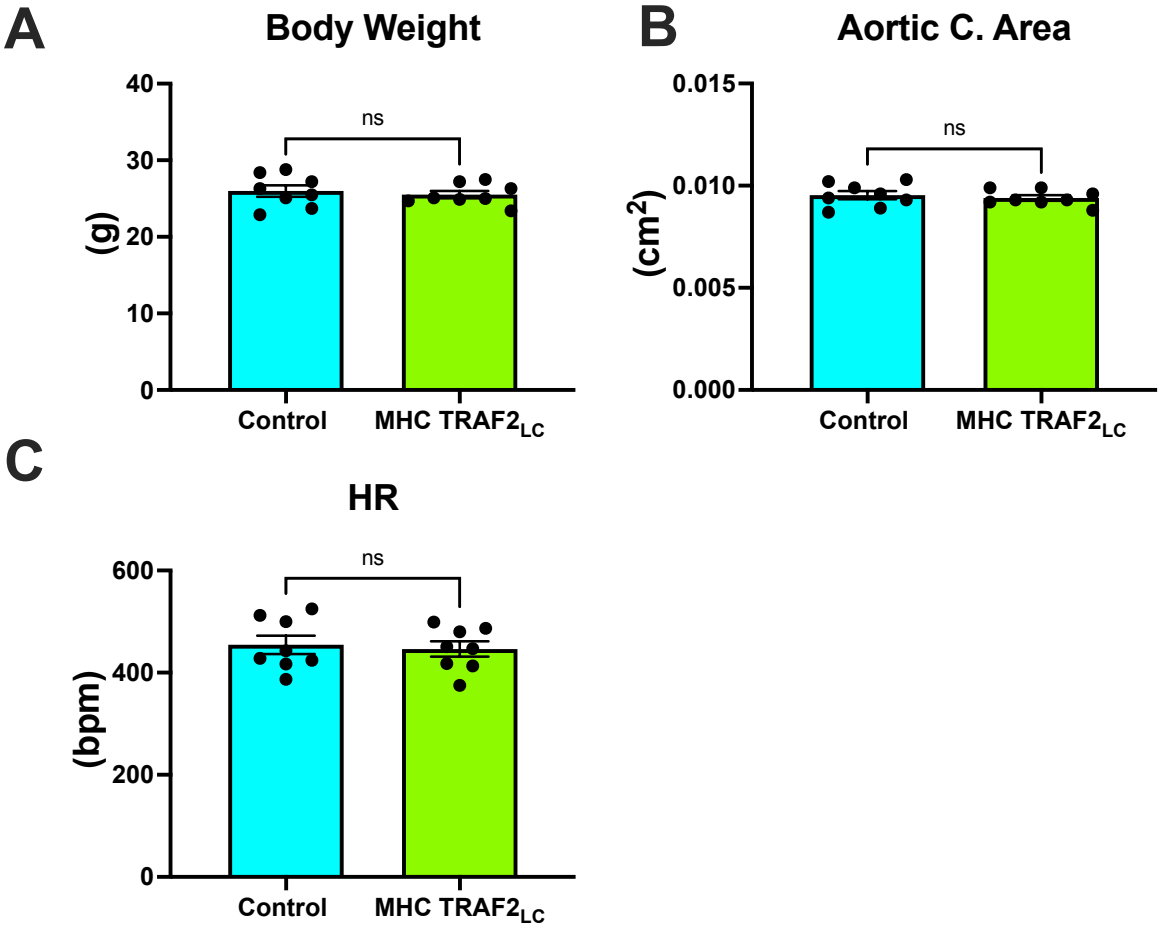
A
Body Weight
(g)
40
30
20
10
0
ns
Control
MHC TRAF2LC
B
Aortic C. Area
(cm2)
0.015
0.010
0.005
0.000
ns
Control
MHC TRAF2LC
C
HR
(bpm)
600
400
200
0
ns
Control
MHC TRAF2LC

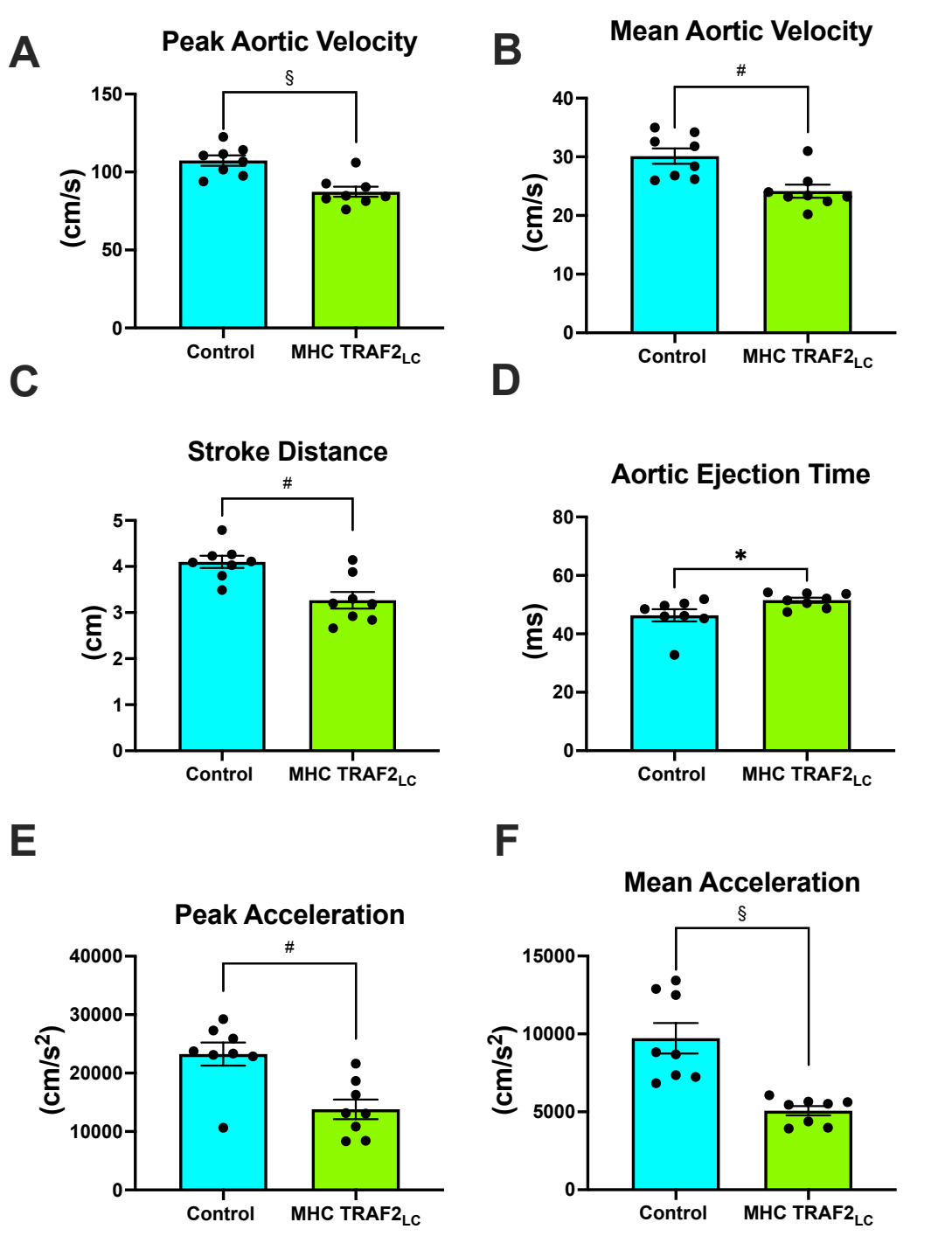
A
Peak Aortic Velocity
§
150
100
50
0
(cm/s)
Control
MHC TRAF2LC
B
Mean Aortic Velocity
#
40
30
20
10
0
(cm/s)
Control
MHC TRAF2LC
C
Stroke Distance
#
5
4
3
2
1
0
(cm)
Control
MHC TRAF2LC
D
Aortic Ejection Time
*
80
60
40
20
0
(ms)
Control
MHC TRAF2LC
E
Peak Acceleration
#
40000
30000
20000
10000
0
(cm/s2)
Control
MHC TRAF2LC
F
Mean Acceleration
§
15000
10000
5000
0
(cm/s2)
Control
MHC TRAF2LC

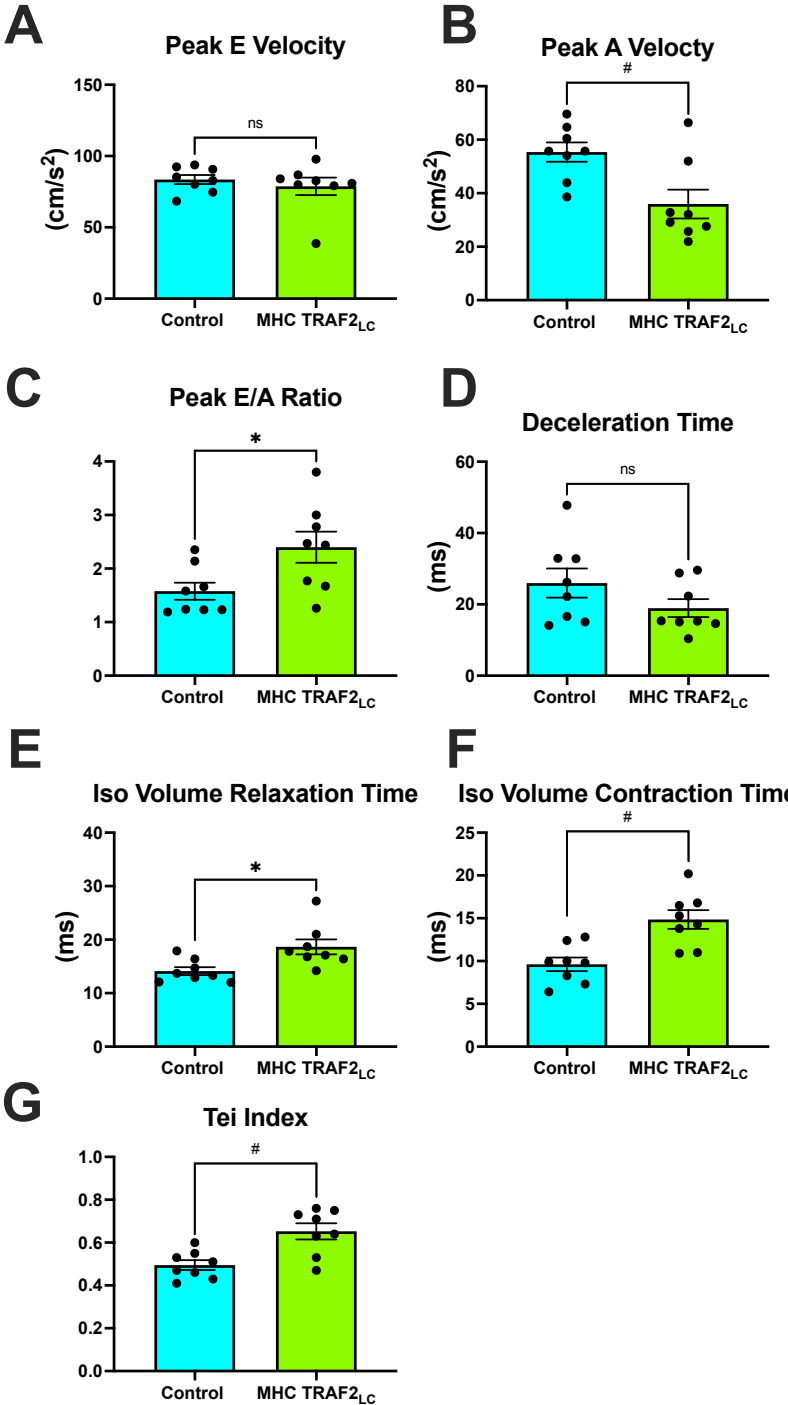
A
Peak E Velocity
(cm/s2)
150
100
50
0
ns
Control
MHC TRAF2LC
B
Peak A Velocty
(cm/s2)
80
60
40
20
0
#
Control
MHC TRAF2LC
C
Peak E/A Ratio
4
3
2
1
0
*
Control
MHC TRAF2LC
D
Deceleration Time
(ms)
60
40
20
0
ns
Control
MHC TRAF2LC
E
Iso Volume Relaxation Time
(ms)
40
30
20
10
0
*
Control
MHC TRAF2LC
F
Iso Volume Contraction Time
(ms)
25
20
15
10
5
0
#
Control
MHC TRAF2LC
G
Tei Index
1.0
0.8
0.6
0.4
0.2
0.0
#
Control
MHC TRAF2LC

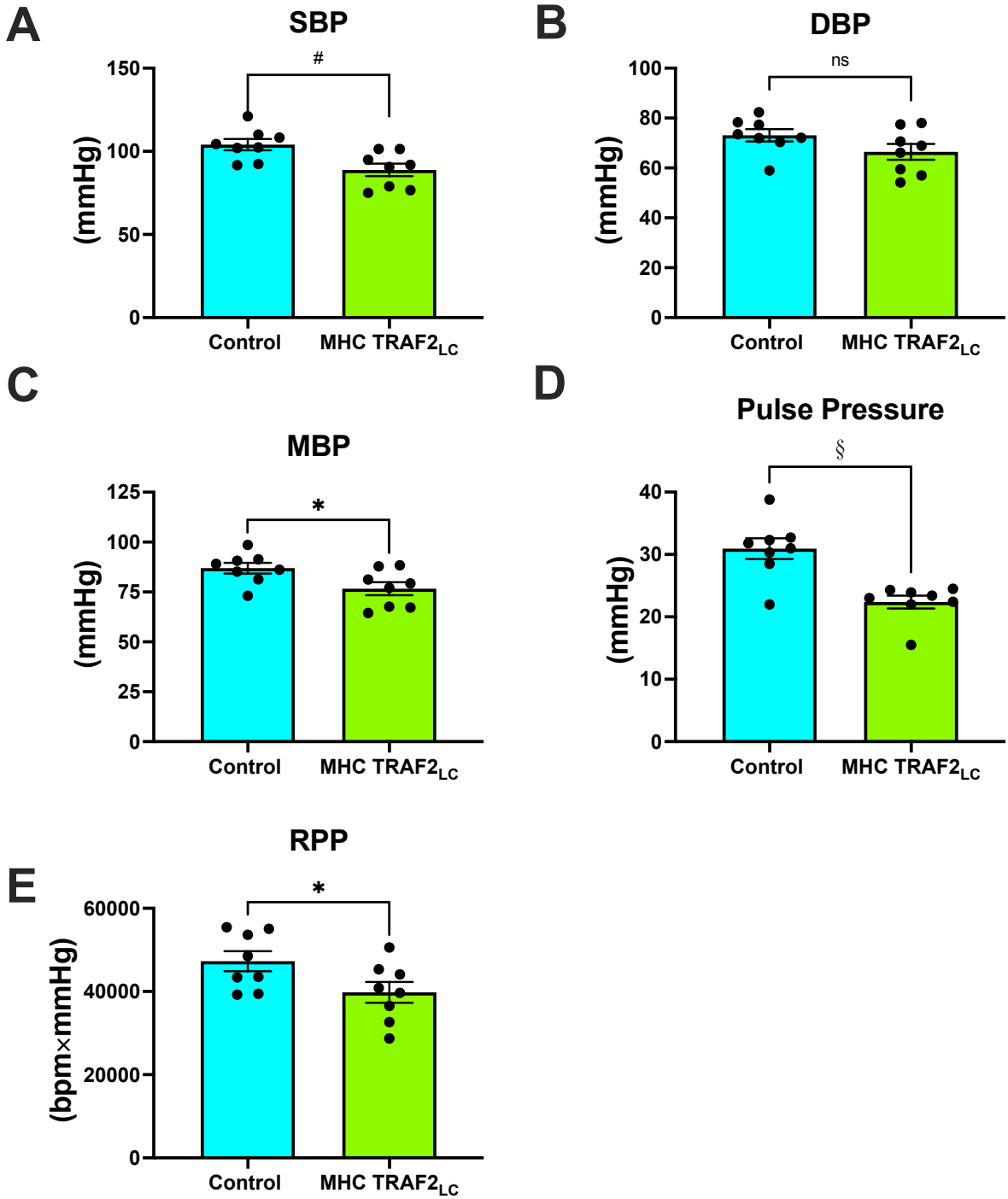
A
SBP
#
150
100
50
0
(mmHg)
Control
MHC TRAF2LC
B
DBP
ns
100
80
60
40
20
0
(mmHg)
Control
MHC TRAF2LC
C
MBP
*
125
100
75
50
25
0
(mmHg)
Control
MHC TRAF2LC
D
Pulse Pressure
§
40
30
20
10
0
(mmHg)
Control
MHC TRAF2LC
E
RPP
*
60000
40000
20000
0
(bpm×mmHg)
Control
MHC TRAF2LC

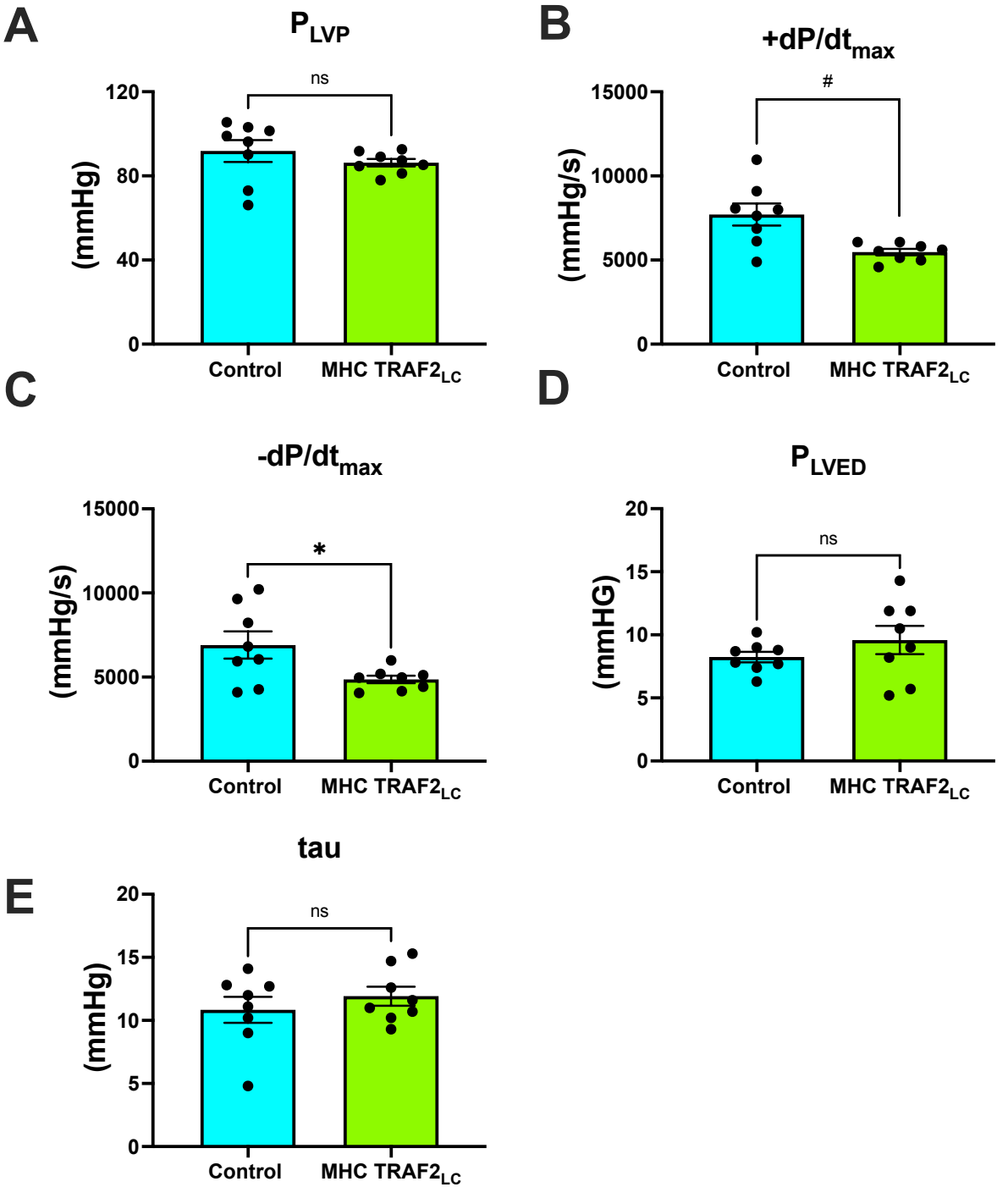
A
P_{LVP}
ns
120
80
40
0
(mmHg)
Control
MHC $TRAF2_{LC}$
B
$+dP/dt_{max}$
#
15000
10000
5000
0
(mmHg/s)
Control
MHC $TRAF2_{LC}$
C
$-dP/dt_{max}$
*
15000
10000
5000
0
(mmHg/s)
Control
MHC $TRAF2_{LC}$
D
P_{LVED}
ns
20
15
10
5
0
(mmHG)
Control
MHC $TRAF2_{LC}$
E
tau
ns
20
15
10
5
0
(mmHg)
Control
MHC $TRAF2_{LC}$

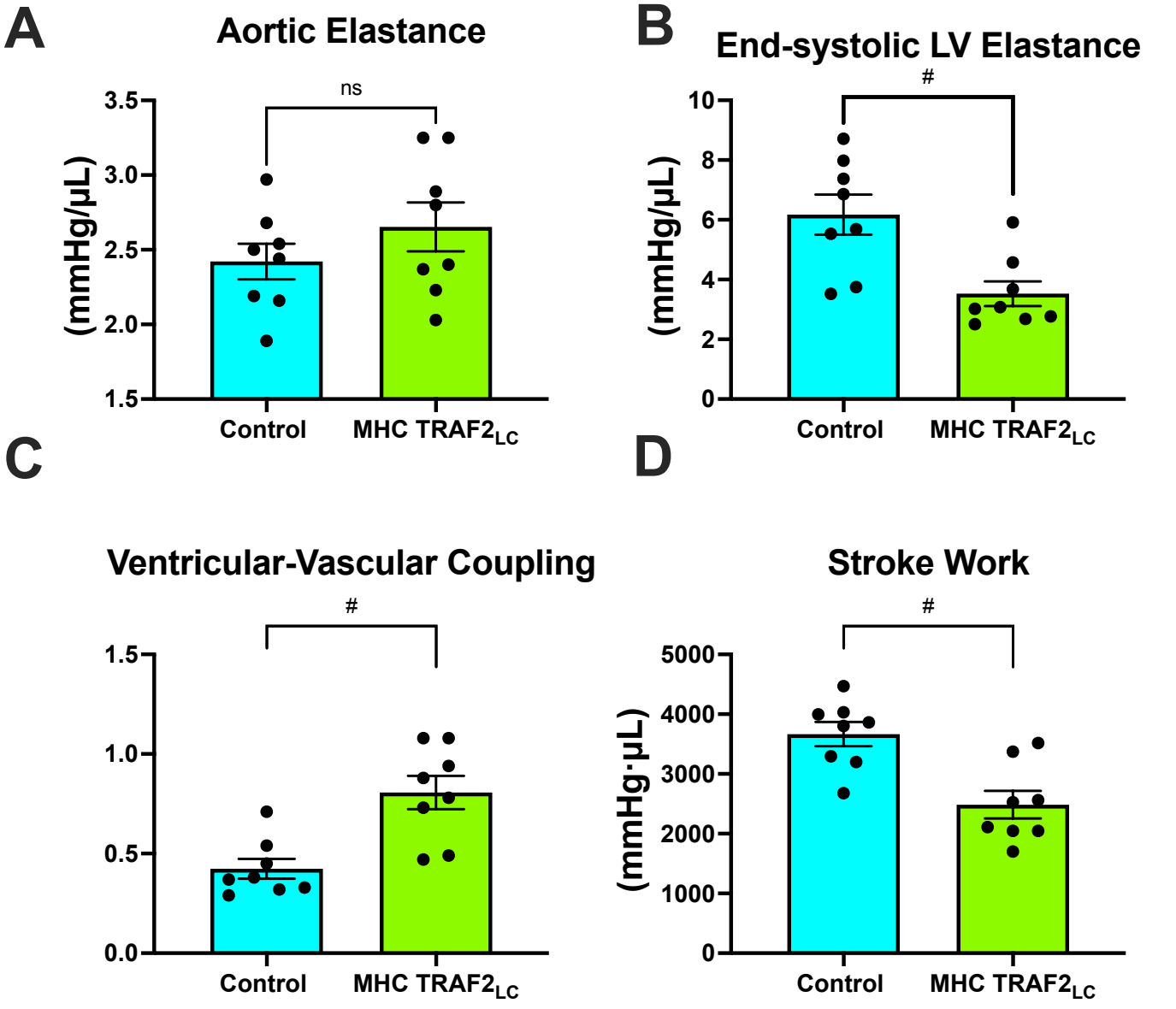
A
Aortic Elastance
ns
(mmHg/µL)
3.5
3.0
2.5
2.0
1.5
Control
MHC TRAF2LC
B
End-systolic LV Elastance
#
(mmHg/µL)
10
8
6
4
2
0
Control
MHC TRAF2LC
C
Ventricular-Vascular Coupling
#
1.5
1.0
0.5
0.0
Control
MHC TRAF2LC
D
Stroke Work
#
(mmHg·µL)
5000
4000
3000
2000
1000
0
Control
MHC TRAF2LC

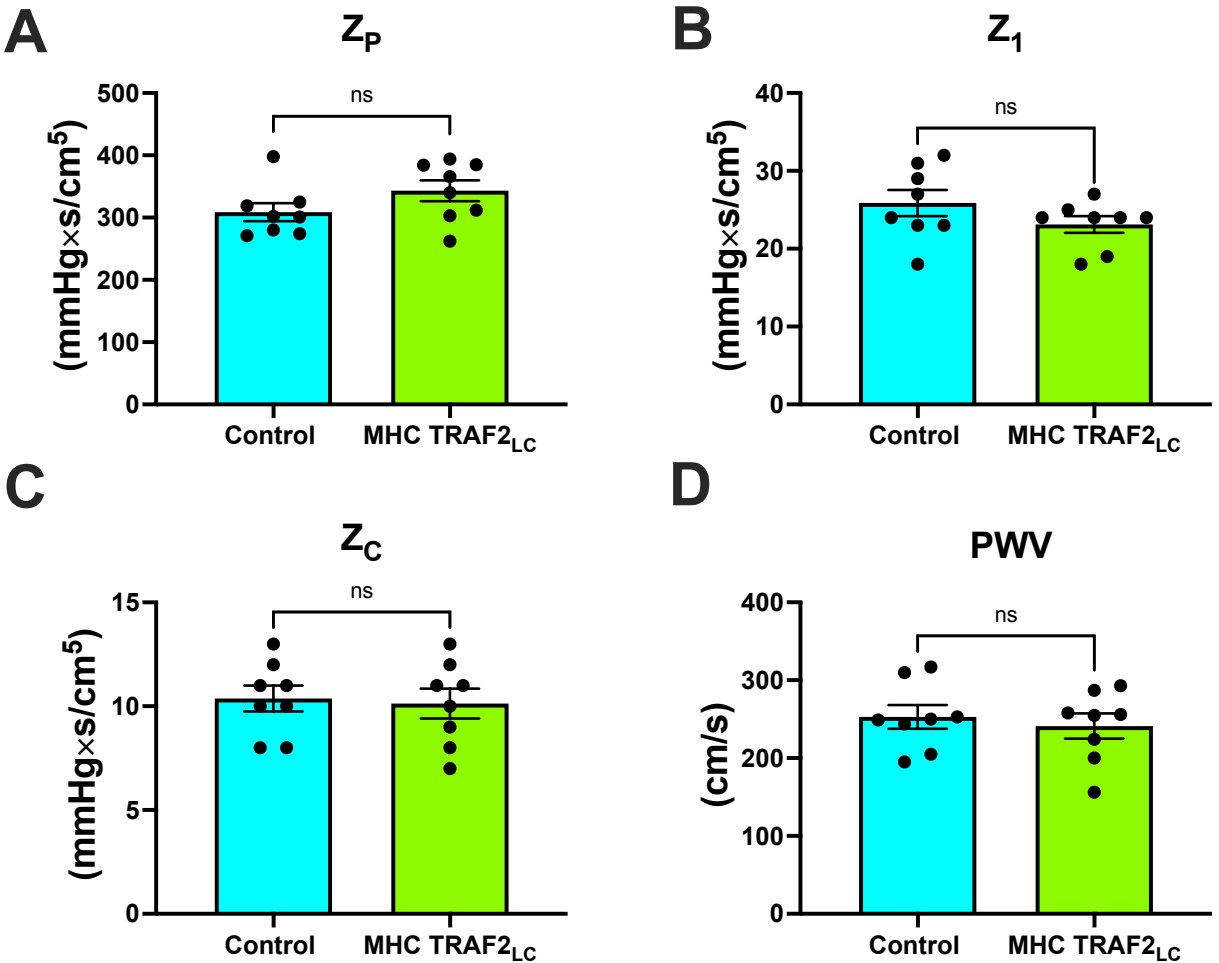
A
Z_P
(mmHg×s/cm^5)
500
400
300
200
100
0
ns
Control
MHC TRAF2$_{LC}$
B
Z_1
(mmHg×s/cm^5)
40
30
20
10
0
ns
Control
MHC TRAF2$_{LC}$
C
Z_C
(mmHg×s/cm^5)
15
10
5
0
ns
Control
MHC TRAF2$_{LC}$
D
PWV
(cm/s)
400
300
200
100
0
ns
Control
MHC TRAF2$_{LC}$